LA-UR -77-1162

TITLE: PASSIVE SOLAR HEATING OF BUILDINGS

AUTHOR(S): J. Douglas Balcomb
James C. Hedstrom
Robert D. McFarland

MASTER

SUBMITTED TO: Workshop on Solar Energy Applications
Associated Universities, Inc.
~~June 27-July 31~~, 1977

, Colorado
May 27-31, 1977

The Los Alamos Scientific Laboratory requests that the publisher identify this article as work performed under the auspices of the USERDA.

los alamos
scientific laboratory
of the University of California
LOS ALAMOS, NEW MEXICO 87545

PASSIVE SOLAR HEATING OF BUILDINGS*

by

J. D. Balcomb, J. C. Hedstrom and R. D. McFarland
Los Alamos Scientific Laboratory
Los Alamos, NM 87545

ABSTRACT

Passive solar heating concepts--in which the thermal energy flow is by natural means--are described according to five general classifications: direct gain, thermal storage wall, solar greenhouses, roof ponds, and convective loops. Examples of each are discussed. Passive test rooms built at Los Alamos are described and results are presented. Mathematical simulation techniques based on thermal network analysis are given together with validation comparisons against test room data. Systems analysis results for 29 climates are presented showing that the concepts should have wide applicability for solar heating.

INTRODUCTION

Solar gains through windows, walls, modified walls, skylights, clerestory windows, and roof sections provide an opportunity to dramatically reduce the total heating energy requirements of a building. When the thermal energy flow is wholly by natural means, such as radiation, conduction, and natural convection, and when solar energy contributes more than half of the total outside energy requirements, then the building is referred to as a passive solar heated structure.

Passive solar heating works very well. This has been demonstrated time and again in a wide variety of buildings located in a wide variety of climates. The occupants of these buildings testify to their comfort, to the ease of their natural operation, and especially to their low fuel bills. A principal problem, however, has been the lack of a quantitative basis for incorporation of the basic concepts into architectural design.

The ERDA Los Alamos Scientific Laboratory has been evaluating passive solar heating for one year under the cognizance of the Division of Solar Energy Heating and Cooling Research and Development Branch. The purpose of the two-year LASL program is to provide the needed quantitative basis for design.

Test rooms have been set up at Los Alamos to study the behavior of passive solar heating elements under carefully controlled conditions. One year of test data have been obtained on a pair of test rooms which utilize thermal storage walls concepts, one with cylindrical water storage tubes and the other with a thick masonry wall. The storage walls are located behind a vertical double-glazed wall. During the mid-winter months each of these rooms has an average inside temperature 60 to 70°F above the ambient temperature. The temperature histories in these rooms are very accurately predicted by simulation analysis techniques developed at LASL.

*Work performed under the auspices of the U. S. Energy Research and Development Administration.

Eleven different buildings have been instrumented in order to study passive solar heating elements within these buildings. These are the Doug Kelbaugh residence in Princeton, NJ, the Benedictine Monastery Dove Publications Building in Pecos, NM, four small buildings at the Ghost Ranch in New Mexico, the Bernardo Chavez solar greenhouse in Anton Chico, NM, the Santa Fe First Village Unit #1, and the residences of Bruce Hunn, Carl Newton, and Tom Shankland in Los Alamos, NM. Data from these installations will be used to validate the simulation analysis technique.

A comprehensive simulation analysis computer code has been written to predict the performance of passive solar heated buildings. The code has been partially validated against test room results and has been used to predict the performance of numerous building geometries. The results of geographic studies done with this code demonstrate that passive solar heating systems can be expected to work effectively in all U.S. climates.

Types of Passive Systems

The first and simplest type of passive system is the *direct gain* approach in which one simply has an expanse of glass, usually double glass, facing south. The building should have a considerable thermal mass, either a poured concrete floor or a massive masonry construction with insulation on the outside. The building becomes a live-in solar collector. The characteristic sun angles result in a good situation since the south face is exposed to a maximum amount of solar energy in the cold winter months when the sun angles are low and a minimum amount of solar energy in the summer when the sun angles are high. Thus the basic seasonal characteristic of control is automatic. An example of this direct gain system is the Wallasey school.[1]

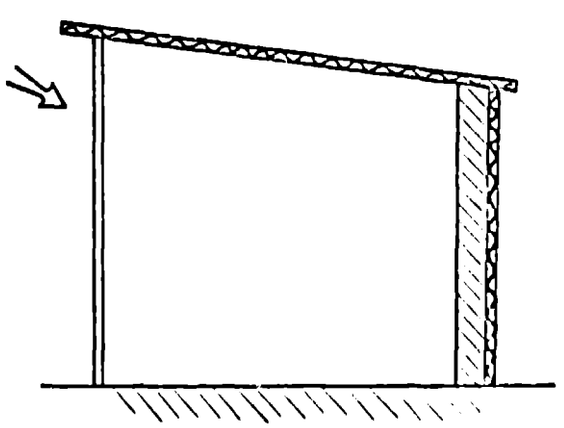

DIRECT GAIN

WALLASEY SCHOOL

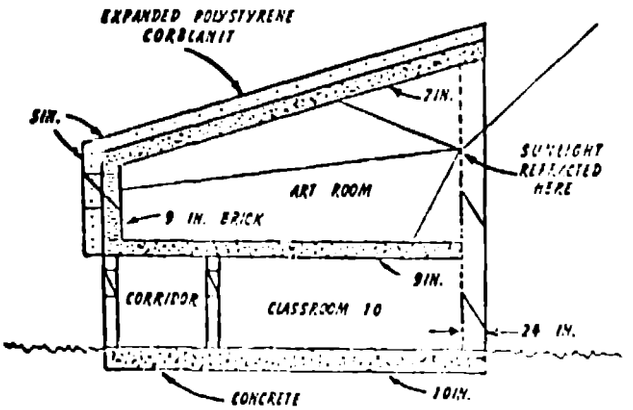

This is certainly the largest passive solar heated structure in the world and one of the first. It was built in 1962, but it is little known. It is a large building of concrete construction with 7 to 10 in. of concrete forming the roof, the back wall, the floor and side walls with 5 in. of expanded polystyrene as the insulation outside of that. The solar wall is a expanse of glass, 27 ft tall and ~ 230 ft long facing south. There are two sheets of glass, the one on the outside is clear and about 2 ft inside of that is a diffusing layer of glass. It is a figured glass, so called, which refracts the suns rays, so that it irradiates the roof and the floor fairly uniformly. This structure is heated to about 50% by the sun, the remaining energy for heating the building comes from the lighting and from the students. The auxiliary system which was originally installed has not been needed. The school is located in Liverpool, England near the sea at a latitude of 53° north.

Another direct gain system is the David Wright house in Santa Fe, New Mexico which uses adobe or earth brick construction with insulation on the outside and has a system of shutters which drop down at night when needed to reduce heat losses.

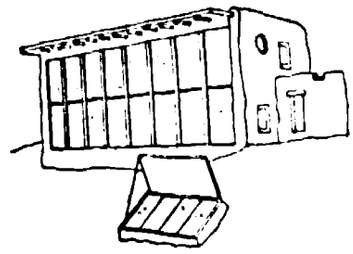

THE DAVID WRIGHT HOUSE

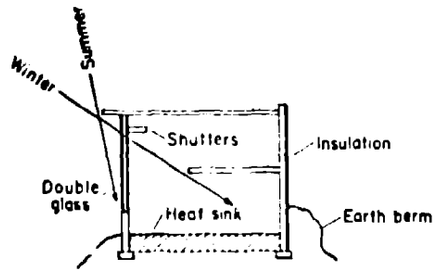

The direct gain approach can take more complicated forms as shown in this sketch by Mark Chalom with the use of clerestory windows or sky lights to provide energy in back rooms.[2]

The second type of system is the *thermal storage wall* in which the thermal storage is in a wall which blocks the sun after it comes through the glazing and stores the heat energy. The wall in this case is usually painted black or a dark color to be a good absorber. It can be water in containers or masonry. A small section of thermal storage wall was used in the Wallassey school discussed earlier.

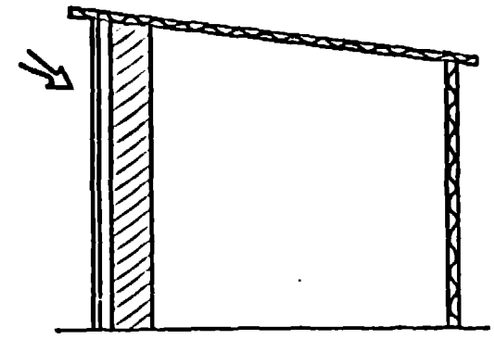

THERMAL STORAGE WALL

An example is the Steven Baer house in Albuquerque, NM in which the thermal storage wall consists of 55 gallon drums filled with water, laid on their side providing a massive thermal storage. A system of

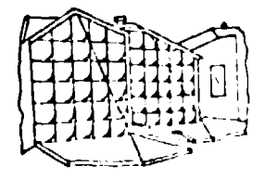

South wall

THE BAER HOUSE

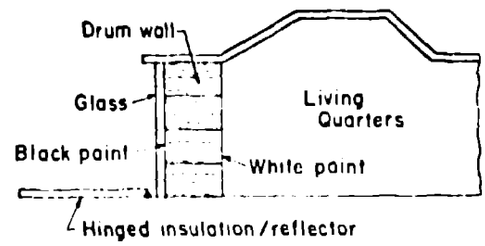

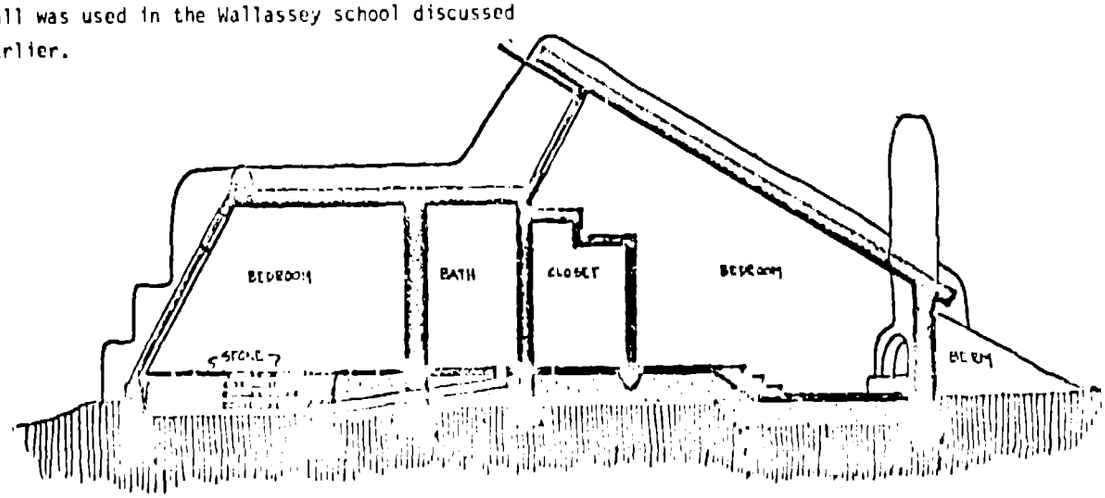

movable insulation is used in which a door forming the south wall lowers during a winter day to allow the sun in and actually reflect some sun onto the storage. There is a single layer of glass. The door can then be raised at night to reduce heat loss.

A very well known implementation of the storage wall concept is the Trombe house in Odeillo, France in which the wall is concrete.[3] In the houses that were built in 1967 the wall is about 2 ft thick. The primary mechanism for heating the house is by radiation and convection from the face of the wall with the thermal energy diffusing through this thick wall. About 30% of the energy is by a thermocirculation path which operates during the day only by natural convection with ports at the bottom and top. Some data taken on this system for a period of four days in December of 1974 are for situations in which the ambient temperature is only slightly above freezing and there are two sunny days, a cloudy day and then another sunny day.[4] The outside surface of the concrete heats up to about 140°-150°F during the day. The inside temperature remains at about 85°F fairly uniform, providing radiant and convective heat to the room

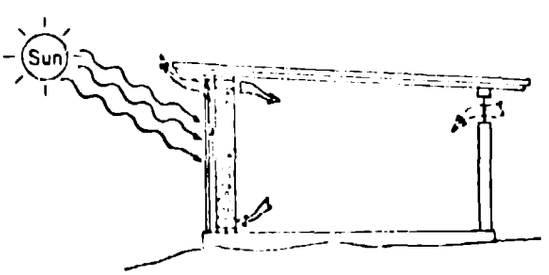

TROMBE HOUSE

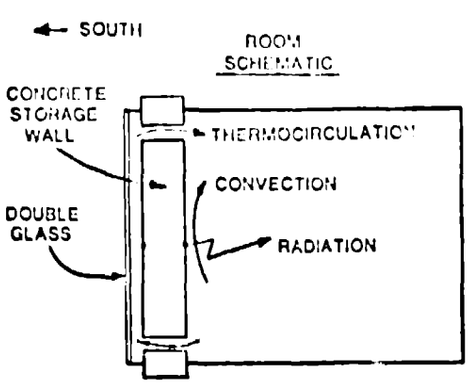

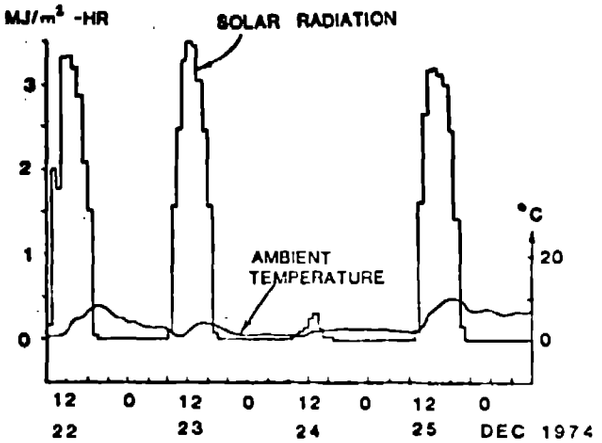

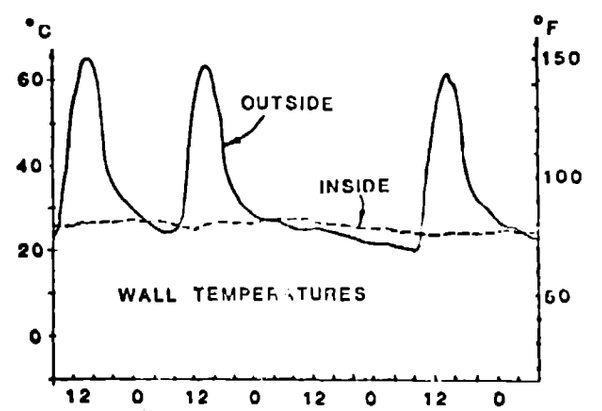

The data taken over a period of one year indicate that about 36% of the total energy incident on the wall is effective in heating the building during the winter months which is typical of a good active solar heating system. About 70% of the total thermal energy required by the building (which is controlled at a temperature of 68°F) was provided by solar energy over this one year period.

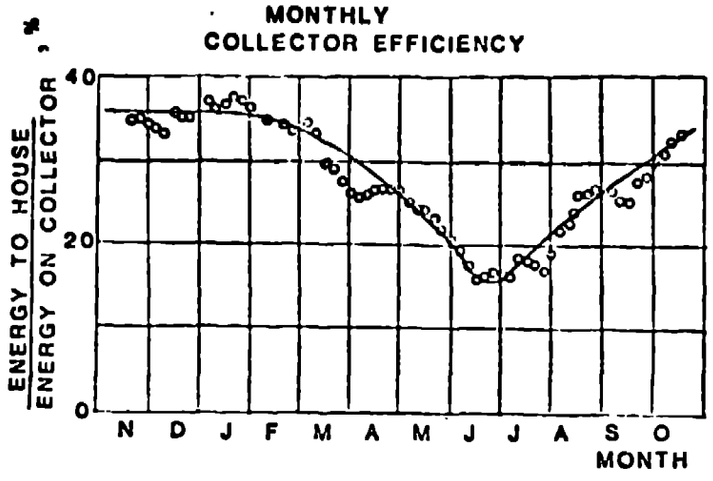

Efficiency of the solar wall of the 1967 Trombe house. Each point represents an average over one month of data.

A mix of these two concepts is the *solar greenhouse* in which one builds a greenhouse onto the south side of a building with some kind of thermal storage wall between the greenhouse and the house. The temperature in the greenhouse does not require very good control as long as the plants do not freeze. Solar energy provides, typically, all of the heat required for the greenhouse as well as providing substantial energy for heating the house.[5]

The fourth type of design is the *roof pond* in which the thermal storage is in the ceiling of the building. In this case movable insulation is needed because the sun angles are altogether wrong. The sun provides large inputs in the summer and small inputs in the winter. It is a good natural cooling system because by using movable insulation one can take advantage of night time radiation. This concept has been implemented in the Atascadero, CA house which uses the Harold Hay skytherm concept.

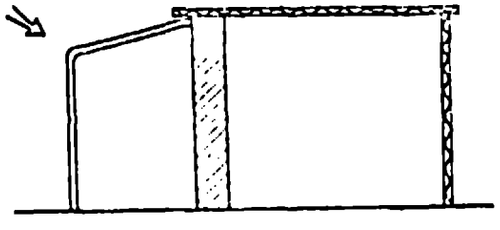

SOLAR GREENHOUSE

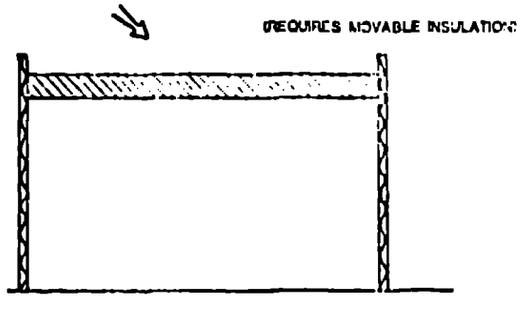

ROOF POND

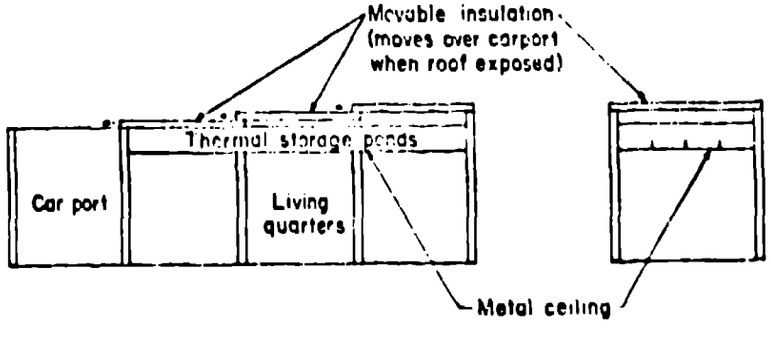

THE HAROLD HAY HOUSE

A system of insulating panels on the roof are is used which slide back and forth on tracks.[6] The water bags are left exposed to the sky during the day in the winter and during the night in the summer. This provides heat input in the winter and heat loss on a summer night. The insulation is put in place during a winter night to conserve heat and during a summer day in order to exclude the sun which is reflected from the top of the white panels. This system has worked very well and has operated without any backup in the rather mild climate of Atascadero providing good thermal comfort in a small building.

The fifth type of passive system is a natural *convective loop*. The classic thermosiphon water heater fits into this category. Natural convective loops which use air as the heat transport fluid have been built and work well. A good example is the Paul Davis house in Corrales, NM.

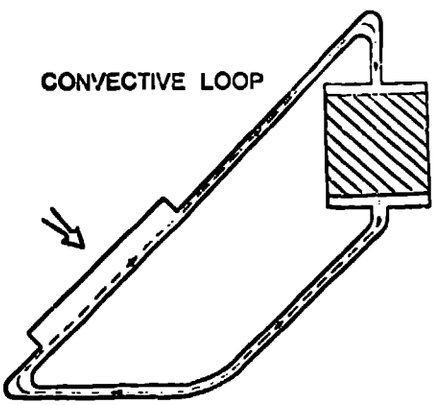

MATHEMATICAL SIMULATION ANALYSIS

Thermal network analysis techniques can be used to predict the performance of passive solar heated buildings. The building temperature state is characterized by 6 to 11 temperatures at various locations--such as air temperature, surface temperatures, glass temperatures, and the temperature of various thermal storage materials at various depths. Energy balance equations are set down for each location accounting for thermal energy transport by radiation, conduction and convection, energy sources from the sun, lights, people, and auxiliary heaters, and sensible thermal energy storage in the material. The temperature history of each location is then simulated by solving these equations for given inputs of solar radiation, ambient air temperature and wind. A one-hour time step is used to march through a one year time period and overall energy flows are accumulated on a monthly basis. This technique is used to characterize the predicted performance of various passive solar heating concepts which use solar gain through windows and thermal storage mass walls. The influence of design is studied by successive computations made with different parameters.

Building Model

The type of thermal network model utilized for the analysis is shown in Fig. 1. This represents a building with a concrete thermal storage wall located behind vertical double glazings. Node 5 represents the temperature of the air between the inner glazing and the wall. Nodes 6 and 11 represent the wall outer and inner surface temperature. The mass of the wall is equally divided between Nodes 7,8,9 and 10 which represent the temperatures within the wall at distances of 1/8, 3/8, 5/8, and 7/8 of the wall thickness from the outer surface. Node 2 represents the room (globe) temperature and Node 1 represents the outside ambient air temperature.

Solar radiation on a horizontal surface, ambient air temperature, and wind velocity are the input variables to analysis, given at hourly intervals. Solar radiation on a vertical surface is calculated by separating the horizontal surface data into direct and diffuse components and applying the proper geometrical transformation as described by Liu and Jordan.[8] A ground reflectance of 0.3 is assumed. The separation of solar radiation into components is done using the technique described by Boes.[9] The transmittance of the glass is calculated as a function of incidence angle using the Fresnel relations and accounting for glass absorptance. The transmittance at normal incidence is 86% per glass layer. The radiation transmitted through the glass is all absorbed at Node 6.

At each hour, node temperatures are calculated as required to achieve an energy balance at the node. Energy storage occurs at only Nodes 7,8,9, and 10.

The thermal energy flow between nodes is calculated based on the temperature difference and the appropriate U-value. The values of U_2, U_4, and U_5 include non-linear radiation terms. All emittances are set at 0.8. The value of U_2 includes a

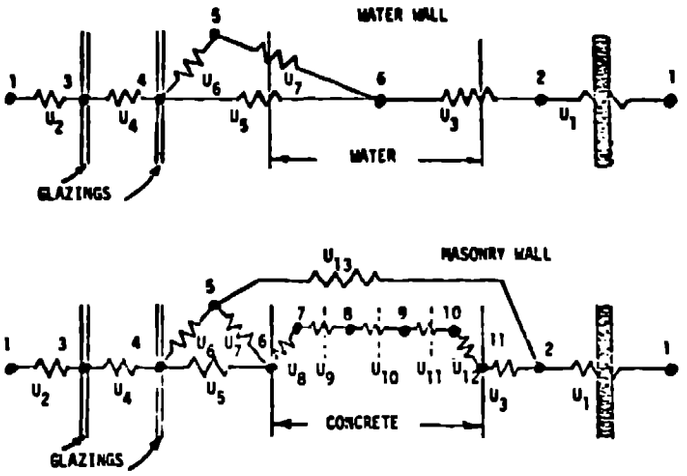

Fig. 1. Simulation schematics of the test rooms.

wind-velocity-dependent convective term. The values of U_3, U_6, and U_7 are a constant 1.0 BTU/hr-°F ft^2. The values of U_8, U_9, U_{10}, U_{11}, and U_{12} represent thermal conduction through the concrete.

In the original version of the masonry thermal storage wall, as developed by Felix Trombe and his colleagues, vent holes are left at the bottom and top of the wall to allow a natural convection air flow from the room floor level up through the space between the inner glass and the wall and return to the room at the ceiling level. This "thermocirculation" provides a mechanism for instantaneous flow of heat into the room during the day. The conductance U_{13} represents this energy flow path. The volumetric air flow is determined from the following relationship:

$$C_d A_v' \sqrt{g\beta|(T_5 - T_2)|/H}$$

where C_d vent discharge coefficient = 0.8,
A_d' = vent opening area per unit width,
= 0.074 ft^2/ft
H = wall height = 8 ft
$\beta = 1/T_5$

Various options are possible as follows:

1) Solid Wall: No thermocirculation is allowed.

2) Trombe Wall: Thermocirculation is allowed only in the normal direction as previously described. Reverse thermocirculation, as would normally occur at night, is not permitted. (This can be implemented with thin plastic film passive damper draped over the inside of the top opening.) It was determined that if reverse thermocirculation is not prohibited then the vents are a net thermal <u>disadvantage</u> to the building.

3) Trombe Wall with Control: The results of the normal thermocirculation frequently is to overheat the building during the day. In this option, the vents are closed whenever the building temperature is 75°F or greater. This greatly reduces the required cooling. This presumably would require some passive or active mechanism.

Another configuration analyzed is the "water wall." This might consist of cans or drums of water stacked to form a thermal storage wall. Alternatively, vertical free-standing cylindrical tubes could be used or any other means of containing water in a thermal storage wall. When heated by the sun on one side the water will freely convect to transport the heat across the wall horizontally and thus temperature gradients across the wall will be very small. The water wall has been analyzed by replacing Nodes 6,7,8,9,10 and 11 in Fig. 1 with a single Node 6 which represents all of the water mass.

In the analysis the room temperature (Node 2) is always maintained within bounds, T_{min} and T_{max}, which are set at 65°F and 75°F, respectively. In the solution of the equations, two possible situations can result:

1) The calculated room temperature falls within the prescribed bounds T_{min} and T_{max}.
2) The calculated room temperature is above T_{max} or below T_{min}.

In the first situation, the room temperature assumes the calculated value. The second situation results in two further possibilities:

1) The calculated room temperature is less than T_{min}. In this instance auxiliary energy is calculated as required to hold the room at T_{min}.
2) The calculated room temperature is greater than T_{max}. In this instance excess heat is dumped (to the environment, presumably by ventilation) in order to hold the room at T_{max}.

The form of the solution is different depending on whether the room temperature is constrained to a bound or floating in-between. In the cases where a transition between operating modes occurs during the hour, the hour is partitioned and the appropriate equations used in each segment.

COMPARISON WITH TEST ROOM RESULTS

The validity of the simulation analysis techniques for two simple concepts is established by demonstrating that they adequately predict the temperature behavior of several small passive test rooms located in Los Alamos, NM. These test rooms are small insulated structures measuring five feet wide by eight feet deep by ten feet high. The south five foot by ten foot exposure is glazed with two sheets of Plexiglas. One test room contains four twelve inch-diameter fiberglass tubes which stand eight feet high directly behind the glass. The tubes are blackened to absorb solar radiation and filled with 188 gallons of water. A second test room contains a 16-inch concrete wall made of stacked cast blocks. Vents at the top and bottom can be opened to allow natural thermocirculation of air. The test rooms are virtually massless except for the thermal storage walls.

On a typical mid-winter clear day (Jan. 11) with an average ambient temperature of 23°F, the water temperature at mid-neight varied from 82°F to 101°F and the room interior globe temperature varied from 74°F to 94°F. Stratification of water temperature of up to 32°F was observed from the bottom of the tube to the top of the tube. In the second test cell, the exterior wall surface temperature varied from 93°F to 153°F, the interior wall surface temperature varied from 84°F to 96°F, the top vent temperature varied from 84°F to 132°F, and the room interior globe temperature varied from 74°F to 98°F. During the longest stormy period of the winter, for which the ambient temperature held at roughly 20°F, the interior temperature of both cells dropped to the yearly minimum of 48°F.

The thermal behavior of both cells is simulated mathematically using a thermal network of 6-11 interconnected points each of which represents a characteristic location within or outside the test cell such as air temperature, surface temperature, glazing temperature, or the temperature of the thermal storage material at some depth within the material. Energy balance equations are written for each location and solved for the hourly observed ambient temperature, solar radiation, and wind conditions. The performance of both test cells can be predicted within roughly ± 2°F under most conditions and about 8°F at the extremes.

An additional 12 test rooms have recently been completed for evaluating various passive concepts. Simulation analysis of these will also be carried out for comparison with observed temperature histories.

Test Room Construction

A plan view of the pair of test rooms is given in Fig. 2. The walls, floor, and ceiling are all 2" x 4" stud-wall construction with 3-1/2" fiberglass insulation. The exterior is covered with plywood sheeting and the interior is lined completely with one-inch polystyrene insulation and all seams are well caulked. Thus the building interior mass is negligible compared with that of the various thermal storage elements added for the tests. The net calculated thermal conduction coefficient (exclusive of the south wall and the common wall) between the building interior and the ambient exterior temperature is 0.23 BTU/°F-hr per square foot of south glazing.

The entire 50 square-foot south wall of each test room is glazed with two sheets of 1/8" Plexiglas sheet separated by a 1/2" air gap. The rooms are actually oriented with the south wall facing 13° east of due south.

Storage Walls

Two different thermal storage wall concepts have been evaluated in the test rooms. The "water wall" consists of four 12"-diameter fiberglass tubes which are free standing behind the glazing separated by 2.4" from one another and the side walls. During most of the winter, these spaces and the two-foot space above the tubes were blocked with 2"-thick polystyrene insulation cut to fit.

The second test room contained a thermal storage wall. An original wall consisting of 8" solid blocks of cinder block was replaced for most of the winter with a 16" wall stacked from 6"x8"x16" blocks of solid cast concrete. Three 3"x8" holes were left open near the bottom and also near the top to allow air to thermocirculate from the room floor level up through the 6" space between the wall and the glazing and return at the room ceiling level. The holes were blocked during portions of the test year, left open day and night during other times, and opened during the day only at other times.

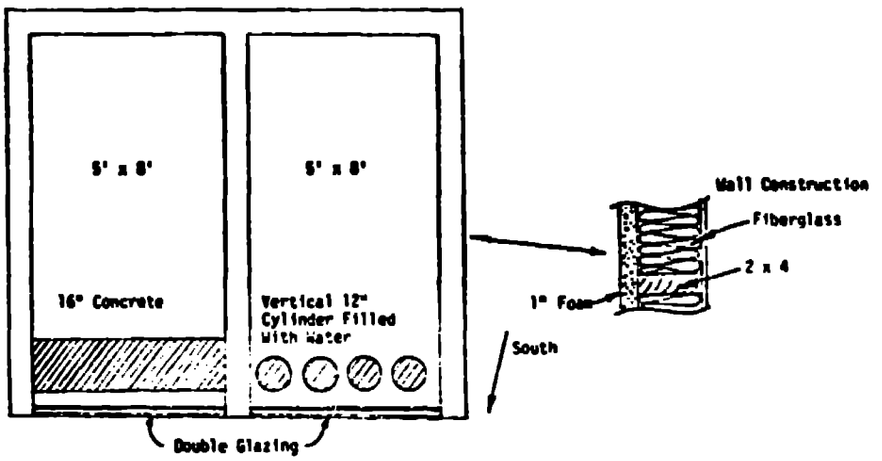

Fig. 2. Plan view of passive test rooms.

Storage masses were as follows:

	Thermal Storage/Glazed Area BTU/°F-ft_g^2
Water-wall	35
Masonry wall	32.5

General Results

The test rooms were very well heated by the sun. Average room temperatures were 60 to 70°F above the ambient average temperature during typical sunny midwinter days. The minimum temperature in the one room was very nearly equal to the minimum temperature in the other room each night throughout the winter. Daily room temperature variations were approximately as follows:

Water wall:	70°F
Masonry wall:	
Vents closed	11°F
Vents open	24°F

Thus the main effect of the thermocirculation vents is to provide direct heat to the room during the day. This increases the daily swing and although the daily average room temperature is larger by about 5°F, it does not noticeably change the minimum room temperature. The maximum inside wall surface temperature occurs at roughly 4:00 p.m. on the water wall and at 8:00 to 10:00 p.m. on the masonry wall.

Simulation Model

Thermal network models of the two test-room configurations are shown in Fig. 1. The thermal conductances used in the analysis are as follows (all values are normalized to one square foot of glazing, ft_g^2): Water wall and masonry wall:

U_1 = "load" = 0.23 BTU/hr°F ft_g^2

U_2 = radiation + exterior film conduction

$$\text{radiation} = \frac{(T_1^2 + T_3^2)(T_1 + T_3)}{1/\varepsilon_1 + 1/\varepsilon_3 - 1}$$

exterior film conduction = 4 BTU/hr°F ft_g^2 (for an average wind speed of 7.5 mph)

α = Stefan-Boltzmann Constant = 1.713×10^{-9} BTU/hr $ft^2°F^4$

ε_1 = 0.8 (Plexiglas)

ε_3 = 0.8 (ambient)

$U_3 = U_6 = U_7$ = 1.0 BTU/hr °F^2 ft_g

U_4 = radiation + conduction

radiation similar to U_2 with $\varepsilon_4 = \varepsilon_5 = 0.8$

conduction = 0.36 BTU/hr °F ft_g^2, (1/2" space)

U_5 = radiation similar to U_2 with $\varepsilon_5 = \varepsilon_6 = 0.8$

Masonry Wall:

$U_8 = U_{12}$ = 4.7 BTU/°F ft_g^2 (2" concrete)

$U_9 = U_{10} = U_{11}$ = 2.35 BTU/°F hr ft_g^2 (4" concrete)

The mass heat capacity of all nodes is zero except as follows:

Water Wall: Node 6 heat capacity = 35 BTU/°F ft_g^2

Masonry Wall: Nodes 7,8,9 and 10 heat capacity = 8.1 BTU/°F ft_g^2

Input to the simulation model are instantaneous hourly values of measured ambient temperature (Node 1) and also the solar radiation measured on a vertical surface parallel to the glazing, integrated over one hour.

Solar transmittance through the glazing is calculated accounting for both Fresnel reflections and for absorption in the glazing based on the calculated incidence angle. This leads to an energy

Figure 3. Comparison for a Period with the Thermocirculation Vents Open.

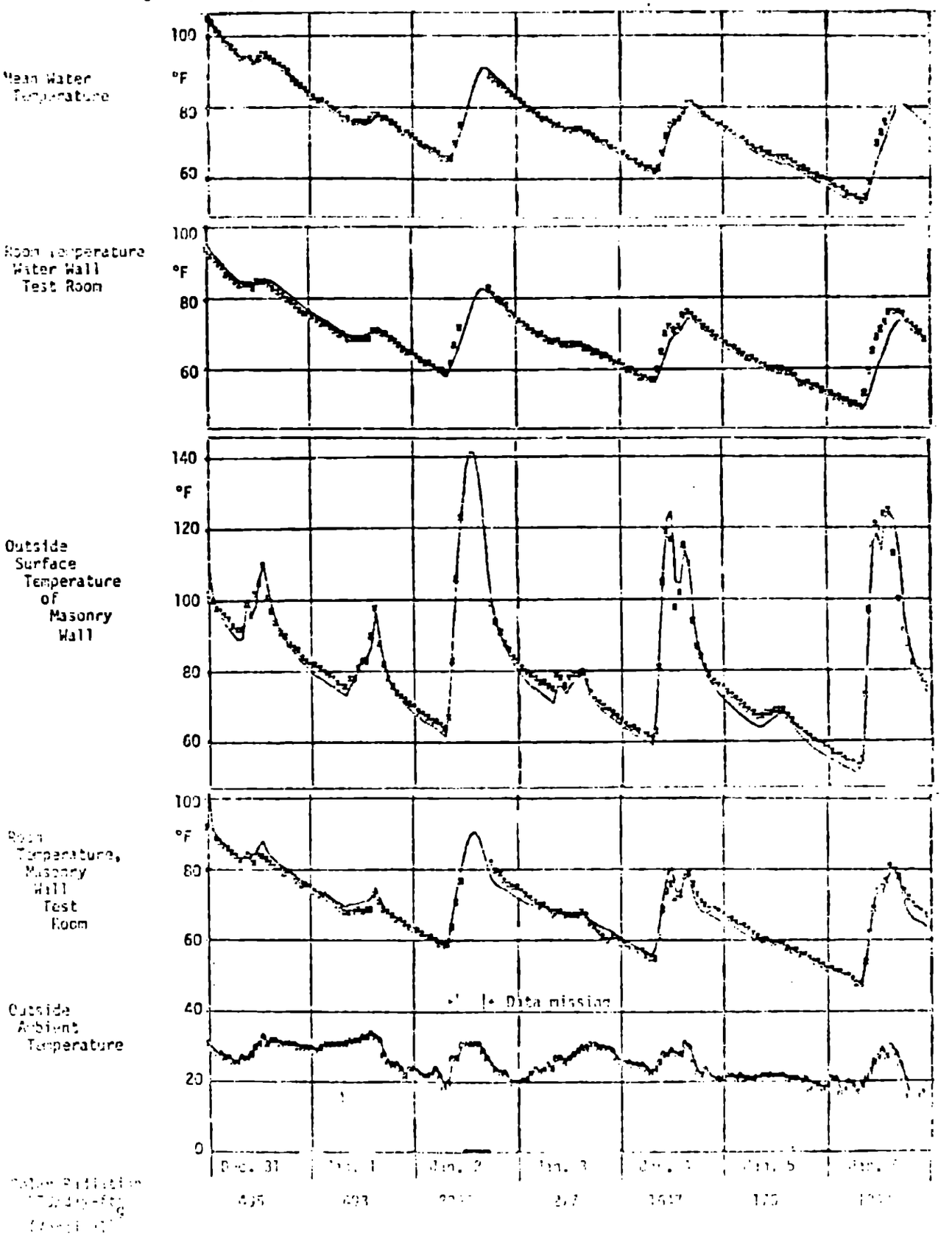

Figure 4. Comparison for a Period with Thermocirculation Vents Closed.

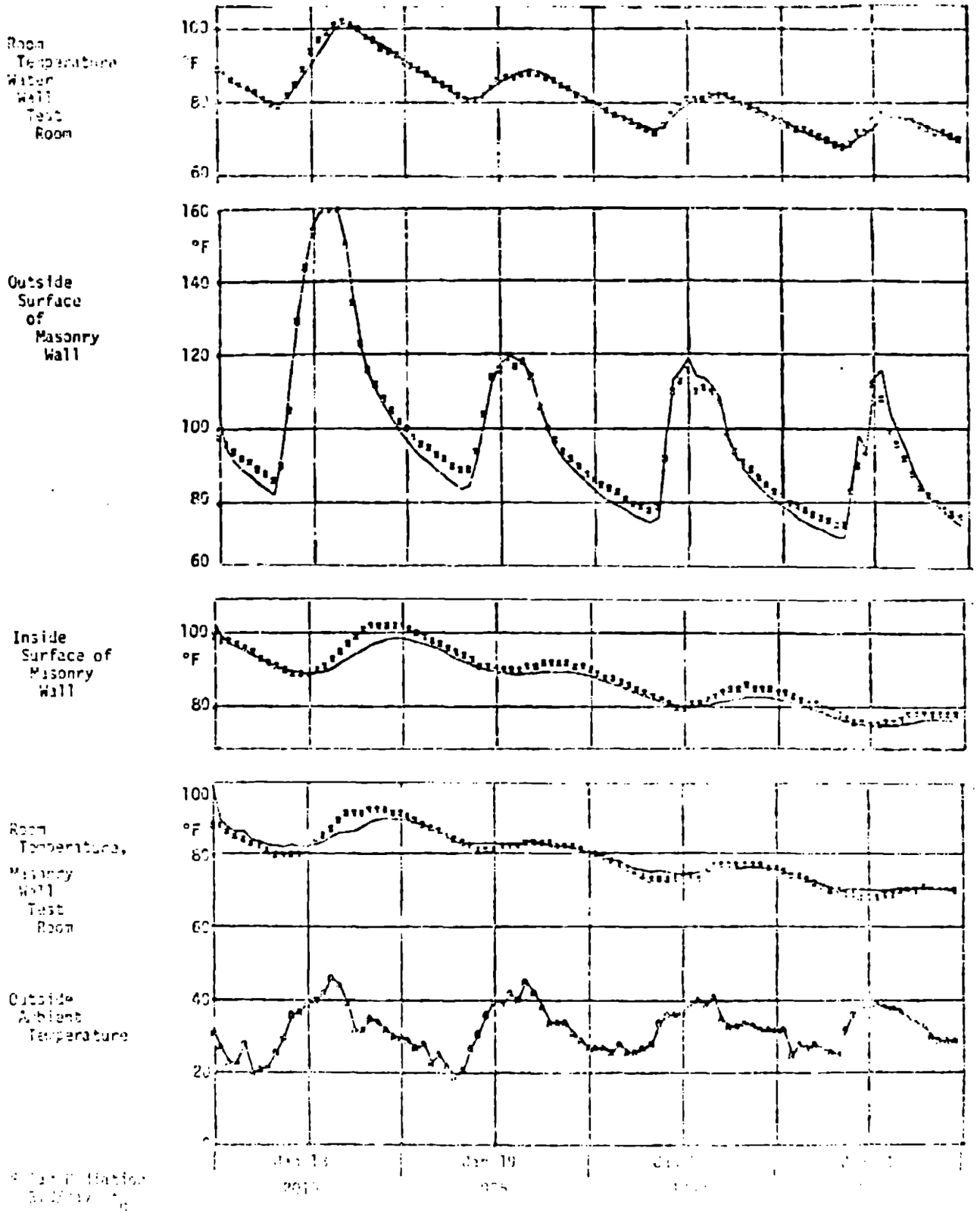

source term into Node 6. For the water wall, 30% of the transmitted solar radiation is reflected out by the light polystyrene blocks between and above the tubes. For the masonry wall this is 20%.

When the vents are open the air flow rate due to thermocirculation is estimated assuming the major flow resistance to be in the vents. The temperature distribution in the wall-glass air space is assumed to be linear so that T_5 is the arithmetic average of the inlet and outlet air space temperatures. The room temperature is assumed to be constant, so the inlet air space temperature is the room temperature, T_2.

When the vents are closed there is no thermocirculation accounted for and all the solar heat transfer to the room is by conduction through the wall.

Temperatures are calculated each hour as required to achieve an energy balance at each node point. Since the thermal conductances are non-linear, this is done by iteration around a linear equation solving routine.

Comparison

Comparison of calculated and measured temperatures have been made for the period December 31, 1976 to January 6, 1977 during which the thermocirculation vents were open and during the period January 18 to 21 when the vents were blocked. The first interval is a period of erratic weather with three separate snowfalls and some bright sunny intervals. The second period starts with a sunny day followed by three days of partial sun.

The simulation model quite accurately predicts the temperature during most of the time--generally within $\pm$ 2°F. The largest errors occur during strong heating periods when discrepancies up to 8°F are observed.

The comparisons are shown on Figs. 3 and 4. For each graph, the symbols * represent the measured quantity and the solid line represents the value calculated by the simulation model.

It is concluded that these particular passive collector-storage elements are quite amenable to accurate representations using the type and level of simulation models employed.

SIMULATION ANALYSIS FOR LOS ALAMOS

For much of the preliminary analysis done to date, the solar and weather data used were for the Los Alamos year September 1972 to August 1973. For this year, the total radiation on a horizontal surface was 518,000 BTU/ft^2 and the space heating load (base: 65°F) was 7350 degree-days (18% higher than normal for Los Alamos). This is a severe test. For these initial studies the glass conductance was characterized by a single constant term rather than the non-linear, two-term representation shown in Fig. 1. The results are useful to determine general effects but the simple model over-predicts the total performance by about 12%. Five different cases have been studied as follows: (see Fig. 5 for designation of symbols).

Case 0: The room and storage are the same temperature. (U_I is infinite.)

Case 1: Storage is coupled thermally only to the room. This case would represent massive internal walls or furniture placed out of the direct sunlight (U_{gs} = 0, U_{ws} = 0).

Case 2: Storage is placed directly in front of the glass. The sun shines on and is absorbed by storage. Storage is thermally coupled to the environment through the glass and also to the room. (U_{gr} = 0, U_{ws} = 0).

Case 3: Storage is placed against the back wall out of the direct sun. This case would represent massive walls or roof insulated on the outside. (U_{gs} = 0, U_{wr} = 0).

Case 4: Storage is placed in the room in the direct sun but loses heat only to the room. (U_{gs} = 0, U_{ws} = 0).

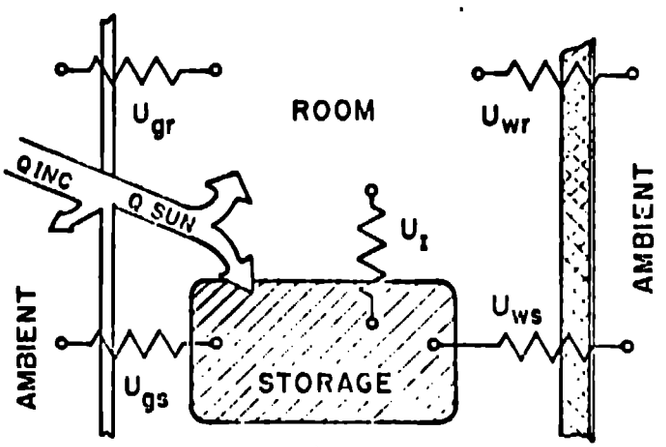

Fig. 5. Passive Solar Heating Model.

These cases are intended to represent extremes. Any real design may tend toward one or another case but will actually be a mixture. For the preliminary study the U values were held constant although in reality, they will vary with temperature difference, wind, and other influences. The glass was assumed to be vertical, to face due south, and to be unshaded. Three glazings were studied:

1) Single glazing: U_g = 1.1 BTU/hr·ft^2-°F.
2) Double glazing: U_g = 0.50 BTU/hr·ft^2-°F
3) Night insulated double glazing: U_g = 0.1, 5 p.m. to 8 a.m.

A value of U_{wr} of 0.5 BTU/hr·ft^2_g-°F was chosen initially.

A storage mass of 30 BTU/ft^2_g-°F was chosen. This is equivalent to 30 lbs of water per sq ft of glass or 150 lbs of concrete.

Lastly the room temperature was allowed to vary 5°F around a desired value of 70°F. Therefore T_{min} = 65°F and T_{max} = 75°F.

Simulation Results for a Case with Isothermal Storage

It is instructive to observe the simulation results for a few days of cold weather. Figure 6 shows the 7-day interval between the 31st of December and the 6th of January. Case 2 was chosen for this calculation with a value of U_3 = 1.0 BTU/hr-ft^2_g-°F. There was snow on New Year's Eve followed by two days of cloudy weather and then cold but sunny weather.

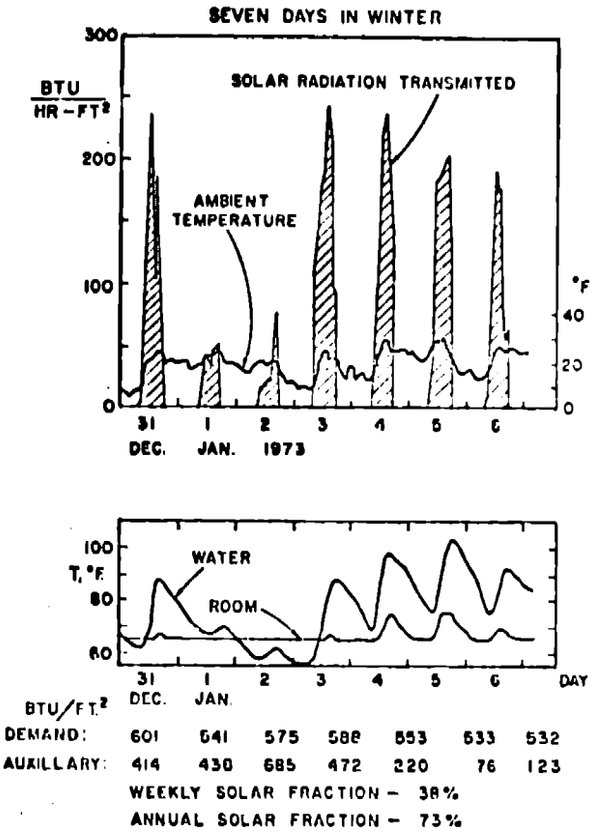

Fig. 6. Seven days in winter, simulation results.

SOLAR PERFORMANCE SUMMARY (CASE 2)

Month	Building Load	Incident Solar Energy on Glass Wall	Solar Energy Transmitted Through Glass Wall	Excess Energy Ventilated	Auxiliary Energy Required	Degree-days (F) (65° Base)	Percent of Solar Heating
	BTU/ft^2 of Glass						
9	6073	36882	25311	6183	48	208	99.20
10	8447	31623	22044	3479	2149	506	74.56
11	13617	40108	29331	638	4300	1032	68.42
12	15006	39693	29638	762	5788	1144	61.43
1	15865	46150	34253	817	4573	1202	71.17
2	13066	38830	27956	961	4053	982	68.98
3	12650	34802	23904	472	5377	980	57.49
4	10451	34283	22682	650	3081	759	70.52
5	6861	30510	19856	2583	842	366	87.72
6	4147	33966	22162	8321	1	123	99.96
7	3520	28398	18686	7413	0	28	100.00
8	3252	31298	20660	8873	0	16	100.00
			Yearly Summary				
	112964	426547	296582	41152	30214	7350	73.25

In the following discussion the effect of variations in various parameters will be shown. In each case the simulation model was run repeatedly varying one parameter at a time while holding the others constant at the nominal values given above. The circled point on each graph represents the nominal case.

Figure 7 shows the yearly results for all five cases as a function of the room-to-storage thermal coupling factor, U_I. All cases become equivalent for large values of U_I. Cases 2 and 4 are observed to be appreciably better in performance than the others. These two cases are for a wall directly heated by the sun. Clearly this is an enormous advantage. Case 4 is unrealistic for low values of U_I because the sun must shine through the room to reach storage and this implies transparent insulation. Case 2 is fairly representative of a "drum-wall," in which the thermal storage is in water contained in cans placed in front of the glass wall.

It is significant to note that there exists an optimum value of U_I for Case 2. The optimum value is approximately 1.5 BTU/hr·°F-ft$_g^2$. The reason for the optimum is as follows. At higher values of U_I, storage loses too much heat to the room during charging periods. This prevents storage from attaining higher temperatures and storing greater amounts of heat. At lower values of U_I, storage attains such high temperatures during charging periods that it loses too much heat through the glass to the environment. Clearly the optimum value of U_I will depend on the chosen storage heat capacity.

The effect of varying storage heat capacity and glass insulation is shown in Fig. 8. Most of the benefits of storage are obtained at a value of 30 BTU/°F-ft$_g^2$. The improvement obtained with double glazing is very dramatic. In fact, a single glazed wall without night insulation can hardly be considered a viable passive solar heating element since only 30% solar heating can be achieved even with large storage and the glass is a net loser at low storage. The increased effectiveness of insulating the glass at night (for example, as in a beadwall) is impressive. The cost-effectiveness of this approach needs further study. Night insulation can be seen to be far more important with single glazing than with double glazing. Single glazing becomes viable only with night insulation. A strategy of placing night insulation based on observed conditions rather than a timeclock would result in only a small increase in performance (~ 2%).

The effect of varying the glass area is inverse to the effect of varying the building thermal load U_w. This is shown in Fig. 9.

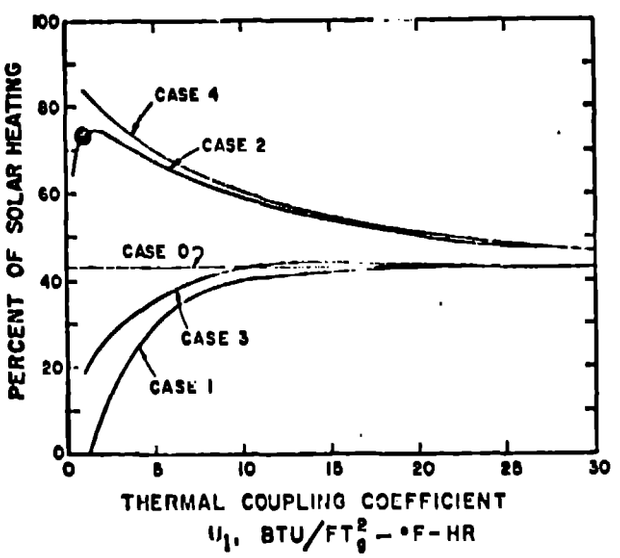

Fig. 7. Effect of thermal coupling between room and storage.

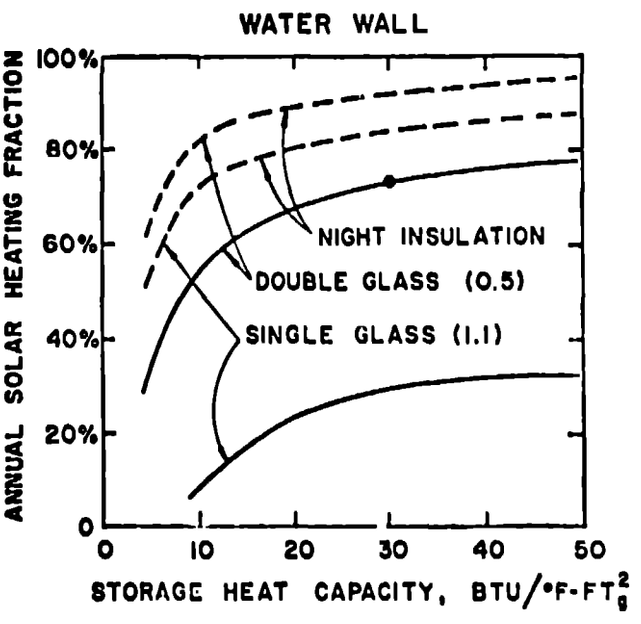

Fig. 8. Effect of storage mass.

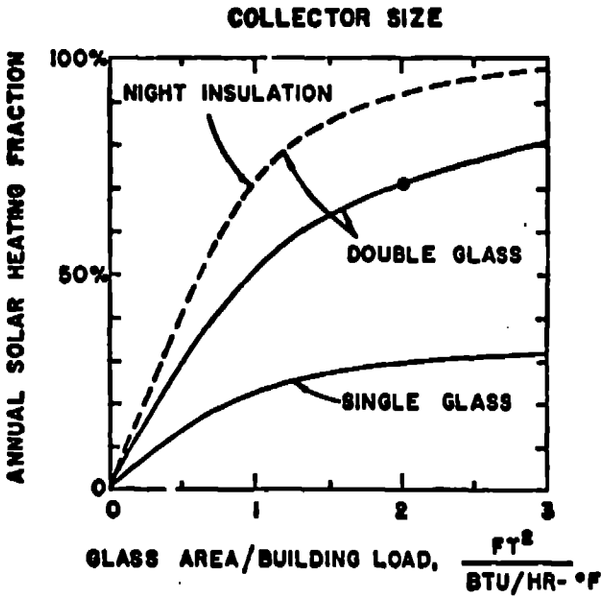

Fig. 9. Effect of glass area.

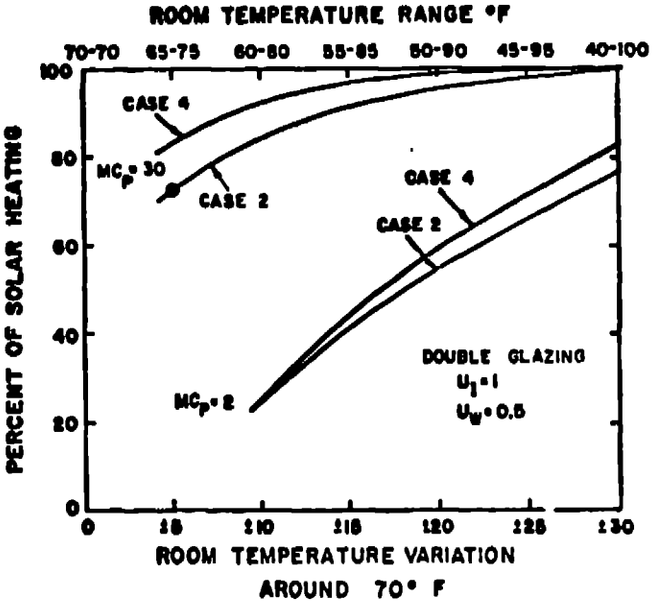

Fig. 10. Effect of allowable room temperature variation.

The effect of the allowable temperature swing is shown in Fig. 10. A variation of ± 5°F may be reasonable for a residence whereas a much larger variation may be tolerable in other buildings such as a warehouse or greenhouse. The effect of mass is also shown for both Cases 2 and 4.

Simulation with a masonry wall

The example of Case 2 is somewhat representative of the concept developed at Odeillo, France by Trombe and his colleagues utilizing a masonry wall, specifically a concrete wall. In the French concept, a thermocirculation path was provided by perforations extending through the wall at the top and bottom. The value of these perforations had not yet been established and this effect was not simulated.

In order to study the basic performance characteristics of such a wall, as compared to the case of an isothermal wall studied earlier, the mathematical model was modified to describe the time and one-dimensional space dependent thermal transport of heat through the wall. This was done by simulation of the masonry temperature at the wall surfaces and at several different distances into the wall.

The thermal properties used for the masonry were as follows (typical of dense concrete):

Heat Capacity: 30 BTU/ft^3 °F
Thermal Conductivity: 1 BTU/ft °F hr

The calculated wall temperatures are shown on Fig. 11a, 11b, and 11c for the same seven-day period shown in Fig. 6 for three different wall thicknesses--0.5 ft, 1 ft, and 2 ft. The daily fluctuations felt on the inside wall surface are markedly different for the three cases, being very pronounced (~ 45°F) for the thin wall and almost non-existent for the thick wall. The longer-term effect of the storm is observed on the inside of the thick wall as a 10°F variation.

The net annual results of several such calculations are summarized in Fig. 12. The net annual thermal contribution of the three different thicknesses of walls are not markedly different. In fact the 1 ft thick wall is the best of the three--giving an annual solar heating contribution of 68%. This compares with a value of 73% for an isothermal wall with the same heat capacity. In each case auxiliary cooling or heating was assumed to maintain the room temperature within the bounds given previously. Although the net thermal contribution of the thin wall and thick wall cases are nearly the same, the amount of control required for the thick wall is much less and the variation in room temperature within the set bounds is much less.

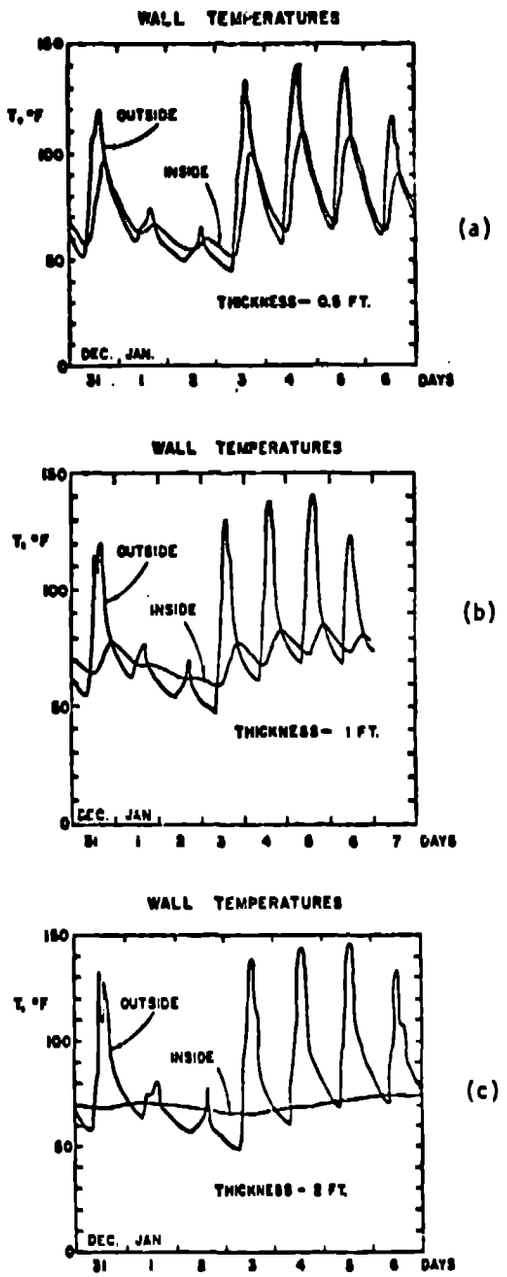

Fig. 11. Time response of a masonry wall for a one-week period.

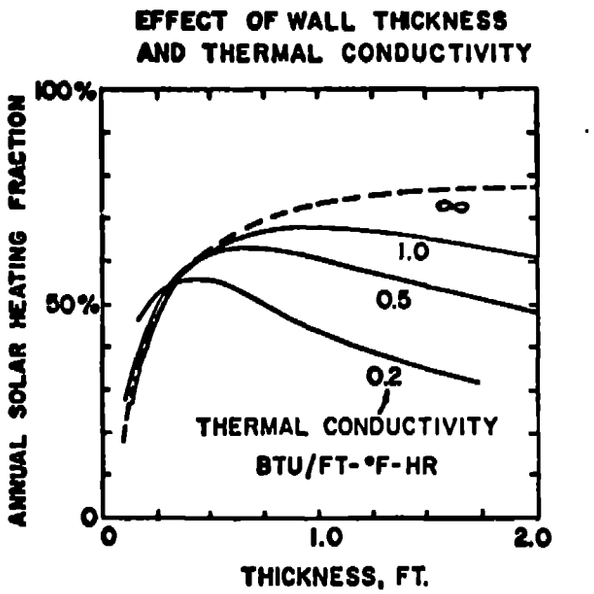

Fig. 12. Yearly performance of a passive masonry wall as a function of thickness for various thermal conductivities.

The effect of variations in wall thermal conductivity is also shown in Fig. 12. The isothermal wall corresponds to the infinite conductivity case. It can be seen that for each conductivity there exists a thickness which will give a maximum yearly solar energy yield. The optimum thickness decreases as the thermal conductivity decreases. Annual heating performance, of course, is only one consideration in the selection of wall materials and wall thickness.

Results for Other Climates

In the analysis for other climates, the more detailed simulation model of the glazing layers was used as shown in Fig. 1. This more accurate representation makes a significant difference--the annual solar heating fraction for Los Alamos was reduced from 68% to 56% in one case. Since the more complex model has been validated against the test room data, it is more to be believed. Several changes in the model are responsible for the change. Probably the most significant is a more detailed accounting of the transmission of diffuse and reflected solar energy.

Hourly values of solar radiation and weather data were obtained from the National Weather Service. A specific one-year period is selected for the hour-by-hour simulation analysis. For Madison, Wisconsin the year chosen is July, 1961 through June, 1962. The results of a parametric study of the effect of thermal storage mass is shown in Fig. 13 for the four cases studied. As had been noted in a previous preliminary analysis, there is an optimum thickness of about one foot for the masonry wall. From calculations done for other locations it is determined that this optimum does not depend on climate.

A study of the effect of climate on performance is given in Table I. These calculations are all for a thermal storage mass of 45 BTU/°F ft_g^2 (~ 18" of concrete or 8.6" of water). Although some cases are clearly better than others, all seem to be viable approaches to solar heating in all the climates studied. The effectiveness of the thermocirculation vents is pronounced in the colder climates.

The ultimate measure of cost-effectiveness of these concepts will be the heating energy delivered to the building by the solar wall. These annual values are given in Table II for the particular case of the 18" Trombe wall.

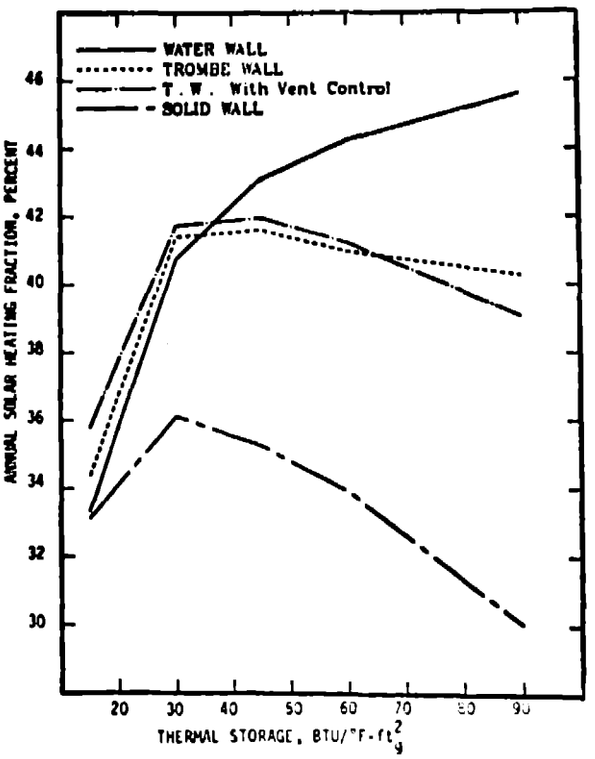

Fig. 13. Effect of storage mass and wall type on the performance of a thermal storage wall passive solar heating system in Madison, Wisconsin. The weather data used are for 1961-62 (7833 degree-days). Load = 0.5 BTU/hr °F ft_g^2.

TABLE I

ANNUAL RESULTS FOR THERMAL STORAGE

= 45 BTU/°F ft_g^2

	Annual Percent Solar Heating				
City	WW	SW	TW	TW(A)	TW(B)
Santa Maria	99.0	98.0	97.9	97.3	98.0
Dodge City	77.6	69.1	71.8	62.8	73.6
Bismarck	49.8	41.3	46.4	31.1	47.6
Boston	60.0	49.8	56.8	44.9	56.7
Albuquerque	90.8	84.4	84.1	81.8	87.5
Fresno	85.5	82.4	83.3	78.0	83.4
Madison	43.1	35.2	41.6	24.7	42.0
Nashville	68.2	60.7	65.2	54.1	65.4
Medford	59.0	53.3	56.1	42.2	56.8

WW: Water Wall
SW: Solid Wall (no vents)
TW: Trombe Wall (no reverse vent flow)
TW(A): Trombe Wall with vents open at all times
TW(B): Trombe Wall with thermostatic vent control

TABLE II

ANNUAL SOLAR HEATING RESULTS FOR 29 VARIOUS CLIMATES

Case: 18 in. Trombe Wall
Thermal Conductivity = 1 BTU/ft hr °F
Heat Capacity = 30 BTU/ft^3 °F
Vent Size = 0.074 ft^2/ft of length (each vent)
No reverse thermocirculation
Load (U_l) = 0.5 BTU/ft^2 °F hr
Temperature band = 65°F to 75°F

City	Year Starting	Heating Degree-Days	Latitude	Solar Heating,* BTU/ft^2_g	Solar Heating Fraction, Percent
Los Alamos, NM	9/1/72	7350	35.8	60,200	56.5
El Paso, TX	7/1/54	2496	31.8	50,000	97.5
Ft. Worth, TX	7/1/60	2467	32.8	38.200	80.8
Madison, WI	7/1/61	7838	43.0	44,900	41.6
Albuquerque, NM	7/1/62	4253	35.0	63,600	84.1
Phoenix, AZ	7/1/62	1278	35.5	38.300	99.0
Lake Charles, LA	7/1/57	1694	30.1	34,300	90.5
Fresno, CA	7/1/57	2622	36.8	43,200	83.3
Medford, OR	7/1/61	5275	42.3	47,400	56.1
Bismarck, ND	7/1/54	8238	46.8	53,900	46.4
New York, NY	6/1/58	5254	40.6	48,000	60.2
Tallahassee, FL	7/1/59	1788	30.3	40,700	97.3
Dodge City, KS	7/1/55	5199	37.8	58,900	71.8
Nashville, TN	7/1/55	3805	36.1	39.500	65.2
Santa Maria, CA	7/1/56	3065	34.8	69,800	97.9
Boston, MA	7/1/57	5535	42.3	47,100	56.8
Charleston, SC	7/1/63	2279	32.8	47,900	89.3
Los Angeles, CA	7/1/63	1700	34.0	53.700	99.9
Seattle, WA	7/1/63	5204	47.5	42,400	52.2
Lincoln, NE	7/1/58	5995	40.8	53,500	59.1
Boulder, CO	1/1/56	5671	40.0	62,500	70.0
Vancouver, BC	1/1/70	5904	49.1	46,000	52.7
Edmonton, ALB	1/1/70	11679	53.5	37,700	24.7
Winnipeg, Man	1/1/70	11490	49.8	33,700	22.6
Ottawa, Ont.	1/1/70	8838	45.3	37,900	31.9
Fredericton, NB	1/1/70	8834	45.8	40,100	33.9
Hamburg, Germany	1/1/73	6512	53.2	24,900	27.5
Denmark	?	6843	56	43,100	43.8
Tokyo, Japan	?	3287	34.6	50,300	85.8

*The values in the solar heating column are the net energy flow through the inner face of the wall into the building.

References:

1. M. G. Davies, "The Contribution of Solar Gain to Space Heating," Paper 47-1 in Extended Abstracts of the 1975 International Solar Energy Congress and Exposition, UCLA, Los Angeles, CA, July 28 to August 1, 1975 (unpublished). To appear shortly in Solar Energy (Journal of the International Solar Energy Society). Also see: J. E. Perry, Jr., "The Wallassey School," to be published in the Proceedings of the Workshop and Conference on Passive Solar Heating and Cooling, Albuquerque, NM, May, 1976.

2. P. VanDresser, "Energy Conserving Folk Architecture in Rural New Mexico," ASC/AIA Forum 75 on Solar Architecture, Arizona State University, 1975, pp 12.1-42.

3. F. Trombe, Maisons Solaires, Techniques de l'Ingenieur (3), 1974, C777.

4. F. Trombe, J. F. Roberts, M. Cabanat and B. Sesolis, "Some Performance Characteristics of the CNRS Solar House Collectors," to be published in the Proceedings of the Passive Solar Heating and Cooling Workshop and Conference, Albuquerque, NM, May, 1976.

5. R. Fisher and W. F. Yanda, "Solar Greenhouses," John Muir Press, Santa Fe, NM. (1976).

6. "Research Evaluation of a System of Natural Air Conditioning," Cal. Poly. State Univ., Jan., 1975.

7. P. Davis, "To Air is Human," Proceedings of the Workshop and Conference on Passive Solar Heating and Cooling, Albuquerque, NM, May 1976.

8. B.Y.H. Liu and R.C. Jordan, "Availability of Solar Energy for Flat-Plate Solar Heat Collectors," ASHRAE, Low Temperature Engineering Application of Solar Energy, 1967.

9. E. C. Boes, "Estimating the Direct Component of Solar Radiation," paper presented at ISES Congress, Los Angeles, CA, July, 1975.
